PHYSICAL REVIEW C **92**, 031305(R) (2015)

Dipole polarizability of ^{120}Sn and nuclear energy density functionals

T. Hashimoto,[1,*] A. M. Krumbholz,[2] P.-G. Reinhard,[3] A. Tamii,[1] P. von Neumann-Cosel,[2,†] T. Adachi,[4] N. Aoi,[1] C. A. Bertulani,[5] H. Fujita,[1] Y. Fujita,[1] E. Ganioğlu,[6] K. Hatanaka,[1] E. Ideguchi,[1] C. Iwamoto,[1] T. Kawabata,[7] N. T. Khai,[8] A. Krugmann,[2] D. Martin,[2] H. Matsubara,[9] K. Miki,[1] R. Neveling,[10] H. Okamura,[1] H. J. Ong,[1] I. Poltoratska,[2] V. Yu. Ponomarev,[2] A. Richter,[2] H. Sakaguchi,[1] Y. Shimbara,[11] Y. Shimizu,[12] J. Simonis,[2] F. D. Smit,[10] G. Süsoy,[6] T. Suzuki,[1] J. H. Thies,[13] M. Yosoi,[1] and J. Zenihiro[12]

[1]*Research Center for Nuclear Physics, Osaka University, Ibaraki, Osaka 567-0047, Japan*
[2]*Institut für Kernphysik, Technische Universität Darmstadt, D-64289 Darmstadt, Germany*
[3]*Institut für Theoretische Physik, Universität Erlangen, D-91054 Erlangen, Germany*
[4]*Department of Physics, Osaka University, Toyonaka, Osaka 560-0043, Japan*
[5]*Department of Physics and Astronomy, Texas A&M University-Commerce, Commerce, Texas 75429, USA*
[6]*Physics Department, Faculty of Science, Istanbul University, 34459 Vezneciler, Istanbul, Turkey*
[7]*Department of Physics, Kyoto University, Kyoto 606-8502, Japan*
[8]*Institute for Nuclear Science and Technology, 179 Hoang Quoc Viet, Hanoi, Vietnam*
[9]*National Institute of Radiological Sciences, Chiba 263-8555, Japan*
[10]*iThemba LABS, Somerset West 7129, South Africa*
[11]*Cyclotron and Radioisotope Center, Tohoku University, Sendai 980-8578, Japan*
[12]*RIKEN Nishina Center, Wako, Saitama 351-0198, Japan*
[13]*Institut für Kernphysik, Westfälische Wilhelms-Universtät Münster, D-48149 Münster, Germany*

(Received 28 March 2015; revised manuscript received 12 August 2015; published 28 September 2015)

The electric dipole strength distribution in ^{120}Sn between 5 and 22 MeV has been determined at the Research Center for Nuclear Physics, Osaka, from polarization transfer observables measured in proton inelastic scattering at $E_0 = 295$ MeV and forward angles including 0°. Combined with photoabsorption data, a highly precise electric dipole polarizability $\alpha_D(^{120}\text{Sn}) = 8.93(36)\,\text{fm}^3$ is extracted. The dipole polarizability as isovector observable par excellence carries direct information on nuclear symmetry energy and its density dependence. The correlation of the new value with the well-established $\alpha_D(^{208}\text{Pb})$ serves as a test of its prediction by nuclear energy density functionals. Models based on modern Skyrme interactions describe the data fairly well while most calculations based on relativistic Hamiltonians cannot.

DOI: 10.1103/PhysRevC.92.031305 PACS number(s): 21.10.Ky, 25.40.Ep, 21.60.Jz, 27.60.+j

The nuclear equation of state (EOS) describing the energy of nuclear matter as function of its density has a wide impact on nuclear physics and astrophysics [1] as well as physics beyond the standard model [2,3]. The EOS of symmetric nuclear matter with equal proton and neutron densities is well constrained from the ground state properties of finite nuclei, especially in the region of saturation density $\rho_0 \simeq 0.16\,\text{fm}^{-3}$ [4]. However, the description of astrophysical systems as, e.g., neutron stars requires knowledge of the EOS for asymmetric matter [5–8] which is related to the leading isovector parameters of nuclear matter, viz., the symmetry energy (J) and its derivative with respect to density (L) [9]. For a recent overview of experimental and theoretical studies of the symmetry energy see Ref. [10]. In spite of steady extension of knowledge on exotic nuclei, just these isovector properties are poorly determined by fits to experimental ground state data because the valley of nuclear stability is still extremely narrow along isotopic chains [11–13]. Thus one needs observables in finite nuclei specifically sensitive to isovector properties to better confine J and L. There are two such observables, the neutron skin r_{skin} in nuclei with large neutron excess and the (static) dipole polarizability α_D.

The neutron skin thickness $r_{\text{skin}} = \langle r\rangle_n - \langle r\rangle_p$ defined as the difference of the neutron and proton root-mean-square radii $\langle r\rangle_{n,p}$ is determined by the interplay between the surface tension and the pressure of excess neutrons on the core described by L [14,15]. Studies within nuclear density functional theory [16] show for all energy density functionals (EDFs) a strong correlation between r_{skin} and the isovector symmetry energy parameters [17–19]. The most studied case so far is ^{208}Pb, where r_{skin} has been derived from the coherent photoproduction of π^0 mesons [20], antiproton annihilation [21,22], proton elastic scattering at 650 MeV [23] and 295 MeV [24], and dipole polarizability [25]. A nearly model-independent determination of the neutron skin is possible by measuring the weak form factor of nuclei with parity-violating elastic electron scattering [26]. Such an experiment has been performed for ^{208}Pb but the statistical uncertainties are still too large for serious constraints of the neutron skin [27].

A particularly useful experimental observable to constrain the large theoretical uncertainties on J and L is α_D [28] which can determined by a weighted integral over the photoabsorption cross section σ_{abs} [29]

$$\alpha_D = \frac{\hbar c}{2\pi^2}\int \frac{\sigma_{\text{abs}}}{E_x^2}dE_x = \frac{8\pi}{9}\int \frac{dB(E1)}{E_x}dE_x, \qquad (1)$$

*hasimoto@ibs.re.kr; Present address: Rare Isotope Project, Institute for Basic Science, 70, Yuseong-daero, 1689-gil, Yuseong-gu, Daejeon, Korea.
†vnc@ikp.tu-darmstadt.de

where E_x is the excitation energy and $B(E1)$ the reduced electric dipole transition strength. It is the aim of this Rapid Communication to present a new experimental result for α_D in a heavy nucleus, ^{120}Sn. This data point is then used together with the well-established $\alpha_D(^{208}\text{Pb})$ to scrutinize EDFs.

The $E1$ response is dominated by excitation of the isovector giant dipole resonance (IVGDR) well known in many nuclei from photoabsorption experiments. Because of the inverse energy weighting in Eq. (1), α_D also depends on the low-energy strength studied mainly with the (γ,γ') reaction. However, extraction of the $E1$ strength from (γ,γ') data is rather model dependent [30].

Recently, polarized inelastic proton scattering at 295 MeV and at forward angles including 0° has been established as a new method to extract the complete $E1$ strength in heavy nuclei from low excitation energy across the giant resonance region [25]. In this particular kinematics, selective excitation of $E1$ and spin-$M1$ dipole modes is observed. Their contributions to the cross sections can be separated either by a multipole decomposition analysis (MDA) [31] or independently by measurement of a combination of polarization transfer observables (PTA) [25]. Good agreement of both methods was demonstrated for the reference case ^{208}Pb where values of r_{skin} and L derived from $\alpha_D(^{208}\text{Pb})$ conform with results from other methods [32].

All EDFs agree on showing strong correlations between α_D, r_{skin}, J, and L, but the actual predictions of α_D for given J and L values differ considerably. While the result for ^{208}Pb [25] already excluded many older Skyrme interactions, modern Skyrme-Hartree-Fock (SHF) and relativistic mean-field (RMF) models can be brought into agreement, e.g., by changing J, which can be varied over a certain range without deteriorating the fit of the interaction parameters [13]. Experimental information on α_D in other nuclei is therefore essential to further constrain the isovector part of the EDF interaction. We note that some information on $E1$ strength distributions in heavy neutron-rich nuclei is available [33–36] but an extraction of α_D from these results is completely model dependent, in contrast to the data discussed here.

Here, we report on a measurement of the electric dipole response in ^{120}Sn with polarized proton scattering based on a PTA covering excitation energies 5–22 MeV. $E1$ strength in ^{120}Sn below 5 MeV was measured by (γ,γ') [37] and above neutron threshold by (γ,xn) [38–40] experiments. A combination of all available data enables a precise determination of α_D. The $E1$ strength has also been determined from a MDA of the (p,p') cross sections [41] but photoabsorption cross sections had to be included as constraints and therefore the result—in contrast to the PTA—is not independent of these data.

The experiment was performed at the RING cyclotron facility of the Research Center for Nuclear Physics (RCNP), Osaka University, Japan. Details of the experimental technique can be found in Ref. [42]. A polarized proton beam was accelerated to $E_0 = 295$ MeV and scattered protons were momentum-analyzed with the Grand Raiden spectrometer [43] placed at 0° covering an angular and excitation energy range of 0°–2.5° and 5–22 MeV, respectively. An isotopically enriched (98.4%) self-supporting ^{120}Sn foil with a thickness of 6.5 mg/cm^2 served as a target. The beam intensity was 1–2 nA with an average polarization of 0.7.

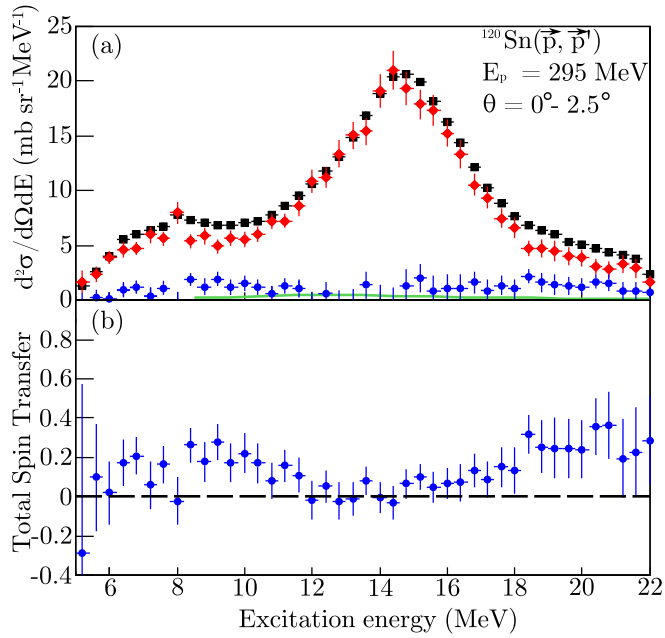

FIG. 1. (Color online) (a) Double differential cross sections (black squares) and decomposition into non-spinflip (red diamonds) and spinflip (blue circles) parts of the $^{120}\text{Sn}(\vec{p},\vec{p}')$ reaction at $E_0 = 295$ MeV and $\theta = 0°$–$2.5°$. The green solid line shows the cross sections due to excitation of the ISGQR estimated as described in the text. (b) Total spin transfer from Eq. (2).

A decomposition of spinflip and non-spinflip cross sections can be achieved [44] by the combined information of the polarization transfer observables D_{LL}, D_{SS}, and D_{NN} [45] determined in a secondary scattering experiment. Since D_{SS} and D_{NN} are indistinguishable at 0°, only D_{LL} and D_{SS} were measured in the present experiment. It is convenient to introduce the total spin transfer

$$\Sigma = \frac{3 - 2D_{SS} - D_{LL}}{4}, \qquad (2)$$

which takes values of zero for non-spinflip and one for spinflip transitions. Because of the different reaction mechanism these can be identified with $E1$ (Coulomb excitation) or $M1$ (spin-isospinflip part of the proton-nucleus interaction) excitations, respectively.

Figure 1(a) displays the measured cross sections (black squares) in 400 keV bins. The bump structure centered at $E_x \simeq 15$ MeV corresponds to the IVGDR. The extracted total spin transfer [Fig. 1(b)] is almost zero in this energy region as expected for Coulomb excitation and approaches maximum values of about 0.2 around 9 MeV (the location of the $M1$ spinflip resonance [46]) and above 18 MeV. The decomposition into non-spinflip and spinflip parts is shown in Fig. 1(a) by red diamonds and blue circles, respectively. The non-spinflip cross sections contain a small $E2$ contribution (green line) from nuclear excitation of the isoscalar giant quadrupole resonance (ISGQR). It was determined using the

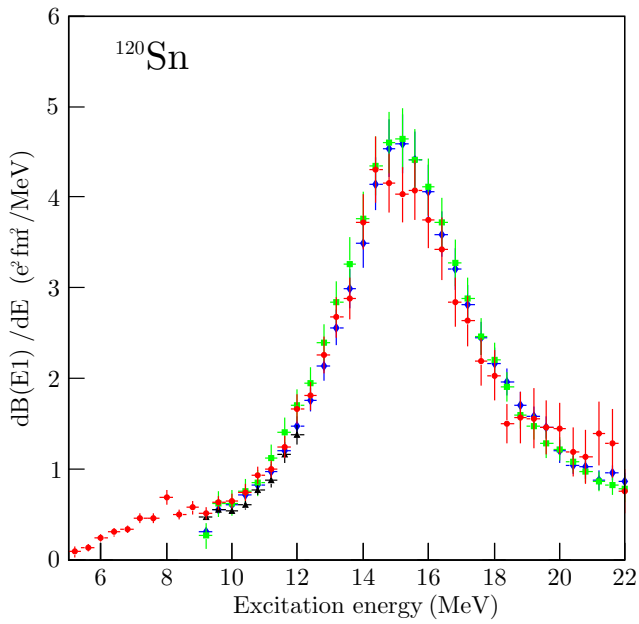

FIG. 2. (Color online) Comparison of the $B(E1)$ strength distribution in ^{120}Sn determined by the present work (red circles) and in (γ,xn) experiments (blue diamonds [38], green squares [39], and black upward triangles [40]).

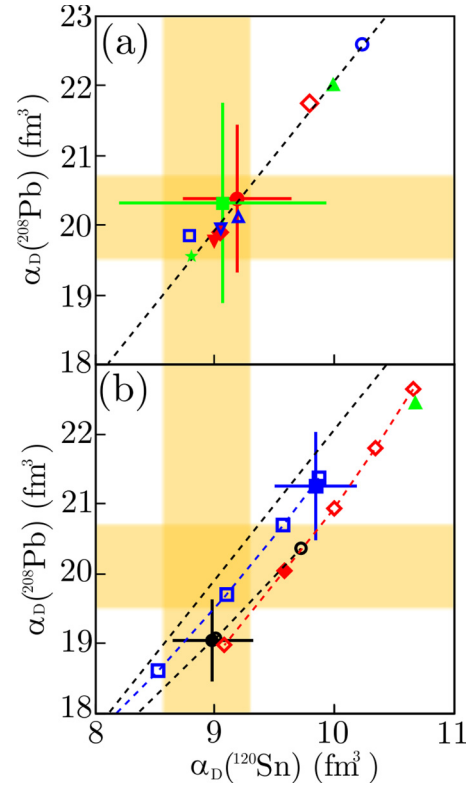

FIG. 3. (Color online) Correlation of the experimental α_D values for ^{120}Sn and ^{208}Pb with uncertainties shown as yellow shaded bands. (a) Comparison with models based on Skyrme interactions SkM* [51] (open red diamond), SkP [52] (open green upward triangle), SkT6 [53] (full red diamond), SG-II [54] (open blue circle), SkI3 [55] (full green upward triangle), SLy6 [56] (full red downward triangle), BSk4 [57] (full green star), SV-bas [13] (open blue downward triangle), and UNEDF2 [58] (open blue square). The SV-min [13] (full red circle) and RD-min [59] (full green square) interactions additionally provide theoretical error bars [13,60]. The dashed black line indicates the correlation between both α_D values. (b) Comparison with relativistic mean field models DD-PC-min [61] (blue squares) and DD-ME-min [62] (black circles), FSU [63] (red diamonds), and FSU2 [64] (green upward triangle). Full symbols denote the results of optimum parameter sets. Open symbols show results varying the symmetry energy parameter J. The dashed lines serve to guide the eye. The dashed black line from (a) is repeated for direct comparison of SHF and RMF models.

isoscalar $B(E2)$ strength distribution [47] as described in Ref. [41] and never exceeds 4% in a single bin.

Figure 2 shows the $B(E1)$ strength distribution (red circles) deduced from the $\Delta S = 0$ cross sections assuming semiclassical Coulomb excitation [48]. The photoabsorption data converted to $B(E1)$ strength are shown as blue diamonds [38], green squares [39], and black upward triangles [40], respectively. All data agree well with each other. Near the IVGDR maximum, slightly smaller values are found in the present work but they still agree with Refs. [38,39] within the experimental uncertainties. Since the MDA analysis below neutron threshold does not depend on the photoabsorption data, the $B(E1)$ strength up to 9 MeV can be compared to the present result. Good agreement of the summed strengths from MDA [48.7(29) e^2 fm^2] and PTA [54.1(41) e^2 fm^2] and the corresponding contribution to α_D is observed.

We now turn to the determination of the electric dipole polarizability in ^{120}Sn taking into account all available data. The energy region below 5 MeV makes a negligible (<0.1%) contribution to α_D [37]. Results for the energy region from 5 to 10 MeV are taken from the present work [49] and amount to 1.12(7) fm^3, contributing about 12.5% to the total value. The main contribution, 7.00(29) fm^3, stems from the IVGDR region, where the present results and those from Refs. [38–40] were averaged between 10 and 22 MeV. Between 22 and 28.9 MeV, data are available from Ref. [38], 0.51(6) fm^3. Finally, the polarizability at even higher energies up to 135 MeV was taken from a $^{\mathrm{nat}}$Sn(γ,xn) experiment [50] neglecting an isotopic dependence. The contribution, 0.31(10) fm^3, is small but non-negligible considering the final precision achieved. In total, we find $\alpha_D(^{120}\mathrm{Sn}) = 8.93(36)$ fm^3, where the error contains the statistical and systematic uncertainties of all data used.

Having now at hand precise data for $\alpha_D(^{120}\mathrm{Sn})$ and $\alpha_D(^{208}\mathrm{Pb})$, we use them to scrutinize the performance of a broad variety of EDFs from SHF and RMF, all values including pairing at the BCS level. The theoretical α_D values are computed from the static response to an external dipole field. Figure 3 displays the EDF results for $\alpha_D(^{208}\mathrm{Pb})$ versus $\alpha_D(^{120}\mathrm{Sn})$ together with the experimental values indicated by yellow shaded bands.

Figure 3(a) collects SHF results for a couple of widely used parametrizations (see caption). Although taken from very different sources, all SHF results together show a strong

correlation between the theoretical α_D values indicated by the dashed black line. The actual position on the line is determined by J and the large span of results along the line demonstrates the uncertainty in J. Note, however, that the majority of SHF results resides nicely within the experimentally allowed yellow square. The outliers are all rather old parametrizations adjusted before appearance of the many data on neutron rich nuclei. The fact that the linear trend goes right through the experimentally allowed square and that most parametrization lies within indicates that the isovector density dependence of SHF is realistic.

Two parametrizations (SV-min, RD-min) are shown together with error bars from statistical analysis [13,60]. These are larger than the experimental uncertainties, demonstrating that the data provide indeed useful constraints on the isovector parameters [12].

Simple error bars hide the linear correlation discussed above. This can be better visualized by a series of parametrizations with systematically varied J [12,13,19]. We do this in connection with RMF approaches shown in Fig. 3(b). Unlike SHF, there is greater variance in modeling density dependence for RMF. We consider three variants thereof: the density-dependent point-coupling model (DD-PC) [61], the density-dependent meson-exchange model (DD-ME) [62], and a non-linear meson coupling model (FSU) [63]. For all three cases we show series with varied J (open symbols) and the best fit (full symbols with error bars where available). For better comparability, the series DD-ME, DD-PC, and RD were fitted to the same data pool as SV-min and RD-min [13]. (Fit procedures for the FSU family are described in Refs. [63,64].) However, the actual fit strategy seems to be of lower importance, because the original standard parametrizations DD-ME2 [62] and PC-1 [61] lie again on the corresponding lines in the plot. All sets are strongly correlated with nearly linear trends, however, with different offsets depending on the form of the EDF. While the SHF series goes approximately through the center of the experimental square, all RMF chains are off center, two of them just touching the square. Only DD-PC comes closer and only one DD-PC parametrization (with $J = 32$ MeV) lies within the correlation box. The best-fit parametrizations (full symbols) are all outside. This indicates that RMF models still need to be improved in the isovector channel [12], although the modern, density-dependent functionals already constitute large progress in this respect in comparison to older RMF functionals [65].

Using the strong correlation between α_D and r_{skin} [28] one can derive the neutron skin thickness of ^{120}Sn from EDFs capable of describing the data in Fig. 3. A similar analysis has been performed for ^{208}Pb [18]. Since the models are not independent, rather than averaging (as done in Ref. [18]) we take the SV-min (red circles) and RD-min (green squares) results as representative and estimate the theoretical uncertainties. Figure 4 shows the predictions of the correlation between r_{skin} and α_D. As for the relativistic models, a variation of J (open symbols) is compatible with the optimum fits (full symbols). The range of values consistent with the experimental polarizability indicated by the horizontal lines corresponds to $r_{skin} = 0.148(34)$ fm. The result is in good agreement with values extracted from measurements of the spin-dipole

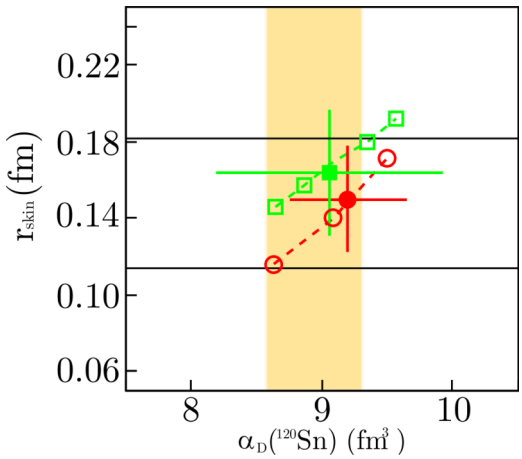

FIG. 4. (Color online) Relationship between α_D and r_{skin} for ^{120}Sn predicted by the SV-min [13] (red circle) and RD-min [59] (green square) interactions. Full symbols are the results of the optimum parameter sets and open symbols correspond to a variation of the symmetry energy parameter J as in Fig. 3(b). Dashed lines are to guide the eye. The horizontal lines denote the range of r_{skin} values compatible with the experimental polarizability shown as a yellow shaded band.

resonance [66], 0.18(7) fm, and proton elastic scattering [67], 0.16(3) fm, while antiproton annihilation [68] finds a much smaller value, 0.08(+3)(−4) fm.

In summary, we have measured polarized proton inelastic scattering off ^{120}Sn at very forward angles and extracted the $E1$ strength distribution between 5 and 22 MeV by an analysis of polarization transfer observables. Combining the present results with (γ,xn) data, the dipole polarizability could be extracted with a precision of 4%. The correlation with the polarizability of ^{208}Pb [25] provides an important test of EDFs indispensable for the extraction of properties of the symmetry energy in neutron-rich matter. Modern Skyrme interactions can describe the data, in contrast to most RMF calculations. With the typical theoretical uncertainties indicated, the combined data from ^{208}Pb and ^{120}Sn provide an important constraint to improve the description of static isovector properties in EDFs.

Considering the importance of polarizability data, a systematic study at different shell closures and exploration of the role of deformation is called for. One important future project is a systematic measurement of α_D covering the range of stable tin isotopes [69]. Together with a new measurement of relativistic Coulomb excitation of the neutron-rich tin isotopes $^{124-134}$Sn at GSI [70] a unique set of data will be available to investigate the impact of neutron excess on the formation of a neutron skin in a set of nuclei with similar underlying structure.

We thank the RCNP accelerator staff for excellent beams. J. Piekarewicz kindly provided us with the FSU and FSU2 results shown in Fig. 3(b). This work was supported by JSPS (Grant No. 25105509), DFG (contracts SFB 634 and NE 679/3-1), and BMBF (contract 05P12RFFTG). N.T. Khai acknowledges support from NAFOSTED of Vietnam under grant 103.01-2011.17.

[1] C. J. Horowitz, E. F. Brown, Y. Kim, W. G. Lynch, R. Michaels, A. Ono, J. Piekarewicz, M. B. Tsang, and H. H. Wolter, J. Phys. G **41**, 093001 (2014).
[2] De-Hua Wen, Bao-An Li, and Lie-Wen Chen, Phys. Rev. Lett. **103**, 211102 (2009).
[3] S. J. Pollock and M. C. Welliver, Phys. Lett. B **464**, 177 (1999).
[4] P. Danielewicz, R. Lacey, and W. G. Lynch, Science **298**, 1592 (2002).
[5] J. Stone and P.-G. Reinhard, Prog. Part. Nucl. Phys. **58**, 587 (2006).
[6] J. M. Lattimer and M. Prakash, Science **304**, 536 (2004).
[7] J. M. Lattimer, Nucl. Phys. A **928**, 276 (2014).
[8] K. Hebeler, J. M. Lattimer, C. J. Pethick, and A. Schwenk, Phys. Rev. Lett. **105**, 161102 (2010).
[9] P. Möller, J. R. Nix, W. D. Myers, and W. J. Swiatecki, At. Data Nucl. Data Tables **59**, 185 (1995).
[10] *Topical Issue on Nuclear Symmetry Energy*, edited by Bao-An Li, A. Ramos, G. Verde, and I. Vidaña, Eur. Phys. J. A **50**(2) (2014).
[11] J. Erler, C. J. Horowitz, W. Nazarewicz, M. Rafalski, and P.-G. Reinhard, Phys. Rev. C **87**, 044320 (2013).
[12] W. Nazarewicz, P.-G. Reinhard, W. Satula, and D. Vretenar, Eur. Phys. J. A **50**, 20 (2014).
[13] P. Klüpfel, P.-G. Reinhard, T. J. Bürvenich, and J. A. Maruhn, Phys. Rev. C **79**, 034310 (2009).
[14] B. A. Brown, Phys. Rev. Lett. **85**, 5296 (2000).
[15] R. J. Furnstahl, Nucl. Phys. A **706**, 85 (2002).
[16] M. Bender, P. H. Heenen, and P.-G. Reinhard, Rev. Mod. Phys. **75**, 121 (2003)
[17] X. Roca-Maza, M. Centelles, X. Viñas, and M. Warda, Phys. Rev. Lett. **106**, 252501 (2011).
[18] J. Piekarewicz, B. K. Agrawal, G. Colò, W. Nazarewicz, N. Paar, P.-G. Reinhard, X. Roca-Maza, and D. Vretenar, Phys. Rev. C **85**, 041302(R) (2012).
[19] J. Erler and P.-G. Reinhard, J. Phys. G **42**, 034026 (2014).
[20] C. M. Tarbert *et al.*, Phys. Rev. Lett. **112**, 242502 (2014).
[21] B. Klos *et al.*, Phys. Rev. C **76**, 014311 (2007).
[22] B. A. Brown, G. Shen, G. C. Hillhouse, J. Meng, and A. Trzcińska, Phys. Rev. C **76**, 034305 (2007).
[23] V. E. Starodubsky and N. M. Hintz, Phys. Rev. C **49**, 2118 (1994).
[24] J. Zenihiro *et al.*, Phys. Rev. C **82**, 044611 (2010).
[25] A. Tamii *et al.*, Phys. Rev. Lett. **107**, 062502 (2011).
[26] C. J. Horowitz and J. Piekarewicz, Phys. Rev. Lett. **86**, 5647 (2001).
[27] S. Abrahamyan *et al.*, Phys. Rev. Lett. **108**, 112502 (2012).
[28] P.-G. Reinhard and W. Nazarewicz, Phys. Rev. C **81**, 051303(R) (2010).
[29] O. Bohigas, N. Van Giai, and D. Vautherin, Phys. Lett. B **102**, 105 (1981).
[30] D. Savran, T. Aumann, and A. Zilges, Prog. Part. Nucl. Phys. **70**, 210 (2013).
[31] I. Poltoratska *et al.*, Phys. Rev. C **85**, 041304(R) (2012).
[32] A. Tamii, P. von Neumann-Cosel, and I. Poltoratska, Eur. Phys. J. A **50**, 28 (2014).
[33] P. Adrich *et al.*, Phys. Rev. Lett. **95**, 132501 (2005).
[34] A. Klimkiewicz *et al.*, Phys. Rev. C **76**, 051603(R) (2007).
[35] O. Wieland *et al.*, Phys. Rev. Lett. **102**, 092502 (2009).
[36] D. M. Rossi *et al.*, Phys. Rev. Lett. **111**, 242503 (2013).
[37] B. Özel-Tashenov *et al.*, Phys. Rev. C **90**, 024304 (2014).
[38] S. C. Fultz, B. L. Berman, J. T. Caldwell, R. L. Bramblett, and M. A. Kelly, Phys. Rev. **186**, 1255 (1969).
[39] A. Leprêtre, H. Beil, R. Bergère, P. Carlos, A. De Miniac, A. Veyssière, and K. Kernbach, Nucl. Phys. A **219**, 39 (1974).
[40] H. Utsunomiya *et al.*, Phys. Rev. C **84**, 055805 (2011).
[41] A. M. Krumbholz *et al.*, Phys. Lett. B **744**, 7 (2015).
[42] A. Tamii *et al.*, Nucl. Instrum. Methods A **605**, 326 (2009).
[43] M. Fujiwara *et al.*, Nucl. Instrum. Methods A **422**, 484 (1999).
[44] T. Suzuki, Prog. Theoret. Phys. **103**, 859 (2000).
[45] G. G. Ohlsen, Rep. Prog. Phys. **35**, 717 (1972).
[46] K. Heyde, P. von Neumann-Cosel, and A. Richter, Rev. Mod. Phys. **82**, 2365 (2010).
[47] T. Li *et al.*, Phys. Rev. C **81**, 034309 (2010).
[48] C. A. Bertulani and G. Baur, Phys. Rep. **163**, 299 (1988).
[49] Photoabsorption data between S_n and 10 MeV are not considered because of potentially large systematic uncertainties close to threshold.
[50] A. Leprêtre, H. Beil, R. Bergère, P. Carlos, J. Fagot, A. De Miniac, and A. Veyssière, Nucl. Phys. A **367**, 237 (1981).
[51] J. Bartel, P. Quentin, M. Brack, C. Guet, and H.-B. Håkansson, Nucl. Phys. A **386**, 79 (1982).
[52] J. Dobaczewski, H. Flocard, and J. Treiner, Nucl. Phys. A **422**, 103 (1984).
[53] F. Tondeur, M. Brack, M. Farine, and J. M. Pearson, Nucl. Phys. A **420**, 297 (1984).
[54] N. Van Giai and H. Sagawa, Phys. Lett. B **106**, 379 (1981).
[55] P.-G. Reinhard and H. Flocard, Nucl. Phys. A **584**, 467 (1995).
[56] E. Chabanat, P. Bonche, P. Haensel, J. Meyer, and R. Schaeffer, Nucl. Phys. A **627**, 710 (1997).
[57] S. Goriely, M. Samyn, M. Bender, and J. M. Pearson, Phys. Rev. C **68**, 054325 (2003).
[58] M. Kortelainen *et al.*, Phys. Rev. C **89**, 054314 (2014).
[59] J. Erler, P. Klüpfel, and P.-G. Reinhard, Phys. Rev. C **82**, 044307 (2010).
[60] J. Dobaczewski, W. Nazarewicz, and P.-G. Reinhard, J. Phys. G **41**, 074001 (2014).
[61] P. W. Zhao, Z. P. Li, J. M. Yao, and J. Meng, Phys. Rev. C **82**, 054319 (2010).
[62] G. A. Lalazissis, T. Nikšić, D. Vretenar, and P. Ring, Phys. Rev. C **71**, 024312 (2005).
[63] B. G. Todd-Rutel and J. Piekarewicz, Phys. Rev. Lett. **95**, 122501 (2005).
[64] Wei-Chia Chen and J. Piekarewicz, Phys. Rev. C **90**, 044305 (2014).
[65] P.-G. Reinhard, Rep. Prog. Phys. **52**, 439 (1989).
[66] A. Krasznahorkay *et al.*, Phys. Rev. Lett. **82**, 3216 (1999).
[67] S. Terashima *et al.*, Phys. Rev. C **77**, 024317 (2008).
[68] R. Schmidt *et al.*, Phys. Rev. C **67**, 044308 (2003).
[69] P. von Neumann-Cosel and A. Tamii, RCNP proposal E422, 2014 (unpublished).
[70] GSI Experiment S412, spokespersons T. Aumann and K. Boretzky (unpublished).